




# A Stellar Ranging Scheme Based on the Second-order Correlation Measurement

Jian Li<sup>1</sup>, Can Xu<sup>1,2</sup> , Yinshen Liu<sup>1</sup>, Yaqi Ma<sup>1</sup>, Xinyao Liu<sup>1</sup>, Xiaochen Ma<sup>1</sup>, Run Fan<sup>1</sup>, and An-Ning Zhang<sup>1</sup>

<sup>1</sup> Center for Quantum Technology Research and Key Laboratory of Advanced Optoelectronic Quantum Architecture and Measurements (MOE), School of Physics,

Beijing Institute of Technology, Beijing 100081, China; [Anningzhang@bit.edu.cn](mailto:Anningzhang@bit.edu.cn)

<sup>2</sup> School of Astronomy & Space Science, Nanjing University, Nanjing 210023, China

Received 2021 July 6; revised 2021 October 20; accepted 2021 November 9; published 2022 January 21

## Abstract

Stellar ranging is the basis for stellar dynamics research and in-depth research on astrophysics. The parallax method is the most widely used and important basic method for stellar ranging. However, it needs to perform high-precision measurement of the parallax angle and the baseline length together. We aim to propose a new stellar ranging scheme based on second-order correlation that does not require a parallax angle measurement. We hope our solution can be as basic as the parallax method. We propose a new stellar ranging scheme by using the offset of second-order correlation curve signals. The optical path difference between the stars and different base stations is determined by the offset of the second-order correlation curve signals. Then the distance of the stars could be determined by the geometric relation. With the distance to stars out to 10 kpc away, our astrometric precision can be better compared to Gaia by simulation. We also design an experiment and successfully demonstrate the feasibility of this scheme. This stellar ranging scheme enables further and more accurate stellar ranging without requiring any prior information or angle measurement.

*Key words:* astrometry – techniques: miscellaneous – methods: observational – methods: miscellaneous – instrumentation: miscellaneous

## 1. Introduction

The determination of stellar distance is the foundation for studying the size, structure and morphology of galaxies. It is also the basis for stellar dynamics research and in-depth research on astrophysics. The development of astronomy is inseparable from the development of ranging. The trigonometric parallax method is undoubtedly the most basic ranging method (Reid et al. 2009, 2014; Zhang et al. 2017; Mignard 2019). As the Earth revolves around the Sun, the observer can see that the star draws a circle or ellipse or line within a year on the celestial sphere depending on the position of the star. The annual parallax of the star can be calculated based on the position of the star separated by two measurements. Methods such as luminosity parallax and mechanical parallax were successively developed based on the trigonometric parallax method. Last century, the Hipparcos satellite released a catalog which contains the positions, parallaxes and proper motions of 117,955 stars with a precision of 0''001 and stellar distances extending out to more than 300 ly. Today, with an astrometric precision of up to 0''00001, Gaia will determine distances to stars out to 30,000 ly away—one hundred times farther than Hipparcos (Smith & Eichhorn 1996; Madore & Freedman 1998; Maíz Apellániz et al. 2018; Gaia Collaboration et al. 2021).

In 1956, Hanbury Brown and Richard Quintin Twiss introduced the second-order correlation of the light field in the measurement of stellar angular diameter (Hanbury Brown 1956). Since then, people have studied the second-order correlation of light field deeply, which opened the field of quantum optics research. In recent years, some researchers studied the ranging technology emitting pseudo-thermal light and measuring the second order correlation coefficient of reflected light (Giovannetti et al. 2001, 2002; Thorn et al. 2004; Giovannetti et al. 2004; Goodman 2007; Zhu et al. 2012, 2013). Just as laser ranging technology needs to emit lasers, this method needs an observer to emit pseudo-thermal light. This method has advantages of high precision, no measured dead zone, strong anti-noise ability, etc. However, this method can only be used for close range and cannot be used for stellar ranging, which is similar to laser ranging technology.

In this paper, we first propose a stellar ranging method based on measuring the second-order correlation of the light field. We can compute the distance difference between multiple observers and the light source by measuring the characteristic peak or dip of the  $g^{(2)}$  curve, and get the baseline distance by laser ranging, finally acquiring the light source distance, as long as the light source does not emit a laser, such as a single photon, thermal light or entangled light. Most stars emit thermal light,

and the full width at half maximum (FWHM) of the  $g^{(2)}$  curve is only dozens of femtoseconds, leading to high accuracy in time measurement (Boitier et al. 2009). Recently, a ghost image using the Sun as a light source was recorded by measuring the  $g^{(2)}$  of Sun, demonstrating the feasibility of measuring the  $g^{(2)}$  of a star (Karmakar et al. 2011; Liu et al. 2014). Simulation results show that our method has a longer range and higher measurement accuracy than the trigonometric parallax method. In our experiment, we produced thermal light, a single photon and entangled light based on the spontaneous parametric down-conversion (SPDC) process (Burnham & Weinberg 1970; Kwiat et al. 1995; Ling et al. 2008; Chang et al. 2014), and carried out the principle demonstration and verification experiment of distance difference measurement, which showed that our results with three kinds of light sources had good consistency in measuring distance, and the measurement accuracy was only constrained by the system's time measurement accuracy.

## 2. Theory

### 2.1. Second-order Correlation Function

The second-order correlation function defined in quantum optics is (Glauber 1963a, 1963b, 1963c; Mandel & Wolf 1995)

$$G^{(2)}(r_1, r_2; t_1, t_2) = \text{tr}[E_1^-(r_1, t_1) \times E_2^-(r_2, t_2)E_2^+(r_2, t_2)E_1^+(r_1, t_1)] \quad (1)$$

where  $E^+(r, t)$ ,  $E^-(r, t)$  represent the positive and negative frequency components of the light field respectively. Normalizing it, we get the following equation

$$g^{(2)}((r_1, t_1), (r_2, t_2)) = \frac{\text{tr}\{\rho E^-(r_1, t_1)E^-(r_2, t_2)E^+(r_2, t_2)E^+(r_1, t_1)\}}{\sqrt{\text{tr}\{\rho E^-(r_1, t_1)E^+(r_1, t_1)\}\text{tr}\{\rho E^-(r_2, t_2)E^+(r_2, t_2)\}}} \quad (2)$$

By analyzing the second-order correlation function of a multi-mode thermal light field, the following equation can be obtained

$$g^{(2)}(\tau^\dagger) = 1 + e^{-(\delta^2\tau^\dagger)^2} \quad (3)$$

in which  $\tau^\dagger = \frac{\Delta}{c} - \tau$ ,  $\Delta$  is the optical path difference from the source to  $r_1$  and  $r_2$ , and  $\tau = t_1 - t_2$  is the time delay. In general, if  $g^{(2)}(\tau^\dagger) > 1$ , the bunching effect of photons manifests. In other words, photons in a thermal state tend to come in pairs.

For particle number state  $|n\rangle$ ,

$$g^{(2)}(\tau^\dagger = 0) = 1 - \frac{1}{n} \quad (4)$$

Obviously it is less than 1. Therefore, the particle number states exhibit an obvious anti-bunching effect. In particular, when the

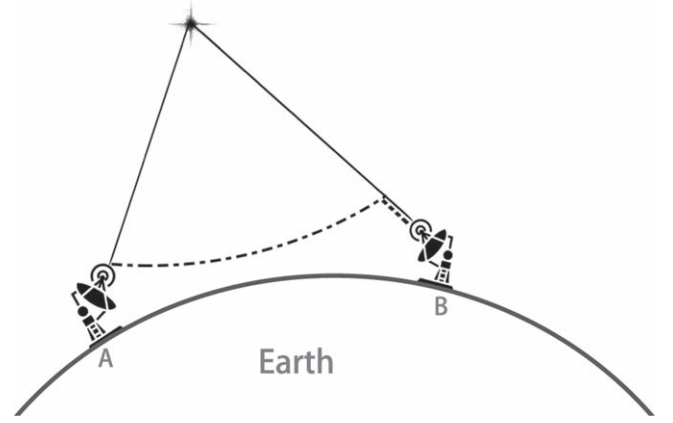


**Figure 1.** Schematic diagram demonstrating acquisition of  $g^{(2)}$  for light from the star. Two observers can both receive light from the star, but there may be an optical path difference (depicted as the dashed line) between them. This optical path difference causes shifting of the  $g^{(2)}$  curve peak along the time axis.

number of photons  $n = 1$ , the single photon state

$$g^{(2)}(\tau^\dagger = 0) = 0. \quad (5)$$

The laser always obeys the following equation

$$g^{(2)}(\tau^\dagger) = 1. \quad (6)$$

The  $g^{(2)}$  curve of the light field can be measured by coincidence counting (Valencia et al. 2002; Gatti et al. 2003).

### 2.2. Ranging Principle

When  $\tau^\dagger = 0$ ,  $g^{(2)}$  of thermal light (or non-classical light) will be maximum (or minimum), therefore, we can use the peak or dip position of  $g^{(2)}(\tau)$  to calibrate  $\Delta$ , the distance of the optical path difference (shown in Figure 1). An example is as follows.

We assume that at the base stations A and B, we detect the light signal from the star separately and measure  $g^{(2)}$ . The results of measurement will be plotted in Figure 2. Signal AA is the  $g^{(2)}$  result of numerical simulation of two observers which are both located at base station A, with no optical path difference or time difference. Signal AB is the  $g^{(2)}$  of two observers respectively located at base stations A and B.

As displayed in Figure 2, when an observer moves from base station A to base station B, the peak position of  $g^{(2)}$  is shifted from the position of AA ( $\tau = 0$ ) to the position of AB. In Figure 2, the peak shifts by  $6 \mu\text{s}$ , that is to say, the arrival time difference of the optical signal is  $6 \mu\text{s}$ . Thus, we obtain the optical path difference  $\Delta = c\tau$  between the star and stations based on the shift of the  $g^{(2)}$  curve's characteristic peak.

From this, we conclude that the abscissa of the  $g^{(2)}$  curve peak (or dip) is 0 only if the arrival time difference between the optical signals of two observers is 0. When there is a difference in the flight time of the optical signal, it is reflected in the  $g^{(2)}$  peak (or dip) shifting left or right. Therefore, we can compute

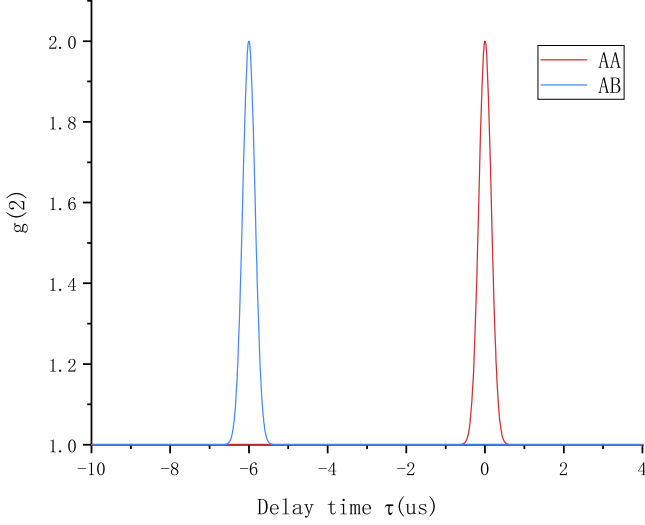


**Figure 2.** An example to illustrate the shifting of  $g^{(2)}$  curve peak. The red curve describes the  $g^{(2)}$  curve for two observers who are both at base station A. The  $g^{(2)}$  peak is at 0 on the time axis because there is no optical path difference between them. The blue one describes the  $g^{(2)}$  curve when observers are located at A and B. The  $g^{(2)}$  peak is at  $-6 \mu\text{s}$  on the time axis, that is to say, the path difference between A and B with respect to the star is  $c * (-6 \mu\text{s})$ .

the optical path difference between the star to each base station from the offset distance of the abscissa of peak or dip, and then get the relationship between the optical distance difference and the distance based on the geometric relationship, so as to achieve stellar ranging. Notably, this method of ranging is not limited by the coherence length. That is because the optical path difference can be compensated using time delay. Therefore, we could set the base station at any place. It is also worth noting that this method does not require accurate angle measurements or parallax calculations, and only requires each base station to collect photons from the stars.

### 2.3. Ranging Method

After the location of the base stations and the second-order correlation information between the base stations are known, the distance and ranging error of the star can be analyzed by considering the geometric relationship. We design a simplified model to show how it works and to discuss the ranging capability of this scheme.

According to the principle that is mentioned in Section 2.2, we propose to establish three base stations A, B and C on the same baseline (as displayed in Figure 3). The length of line segments AB and BC is the distance between each other's base stations respectively, and determined by their locations. But for the convenience of simplified models and simulation, we equalize them and set the value as  $a$  in this paper. The distance from the star to base station A (B or C) is SA (SB or SC). Then the distance difference is  $L_B = SB - SA$  and  $L_C = SC - SA$ . According to the law of cosines, the distance from the star to

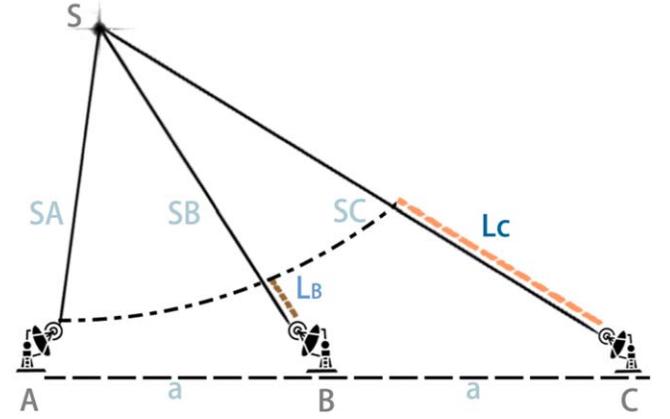


**Figure 3.** Three station ranging method. A, B and C are three base stations on the same baseline where the length of line segment AB and BC are both equal to  $a$ . SA (SB or SC) is the distance from the star to the base station A (B or C).  $L_B = SB - SA$  and  $L_C = SC - SA$  are the differences in distance. If we know  $a$ ,  $L_B$  and  $L_C$ , then SA can be determined by calculation.

the base station A,  $SA=L$ , can be calculated by

$$L = \frac{2a^2 + 2L_B^2 - L_C^2}{2L_C - 4L_B}. \quad (7)$$

In general, baseline distance  $a$  is much less than star distance  $L$ . The baseline distance  $a = \frac{1}{2}c * t_a$  is measured by laser ranging.  $L_B = c * \tau_b$  and  $L_C = c * \tau_c$  can be calculated by measuring the shift of  $g^{(2)}$  curve's characteristic peak. After getting this information, Equation (7) can be written as

$$L = \frac{t_a^2 + 2\tau_b^2 - \tau_c^2}{4\tau_c - 8\tau_b} * c. \quad (8)$$

The above equation indicates that by using the three-station ranging method, only  $t_a\tau_b\tau_c$  need to be measured to achieve stellar ranging, with no need for measuring viewing angle difference between the base stations.

### 2.4. Error Analysis

Assuming that the measurement error of  $t_a\tau_b\tau_c$  totally depends on the precision of time measurement  $\Delta t$ , the following error measurement formula can be obtained

$$\Delta L = \left[ \frac{t_a}{2\tau_c - 4\tau_b} - \frac{t_a^2 + 2\tau_b^2 - \tau_c^2}{4 * (\tau_c - 2\tau_b)^2} - \frac{1}{2} \right] * c * \Delta t. \quad (9)$$

According to formula (9), error estimation can be made via the actual measurement values of  $t_a\tau_b\tau_c$  and the precision of time measurement  $\Delta t$ .

In order to analyze the relationship between the relative error of ranging and various influencing factors, we drew Figures 4 and 5 according to formula (9).

Figure 4 depicts the numerical simulation results of stellar distance  $L$  and relative error with different baseline lengths  $a$ .

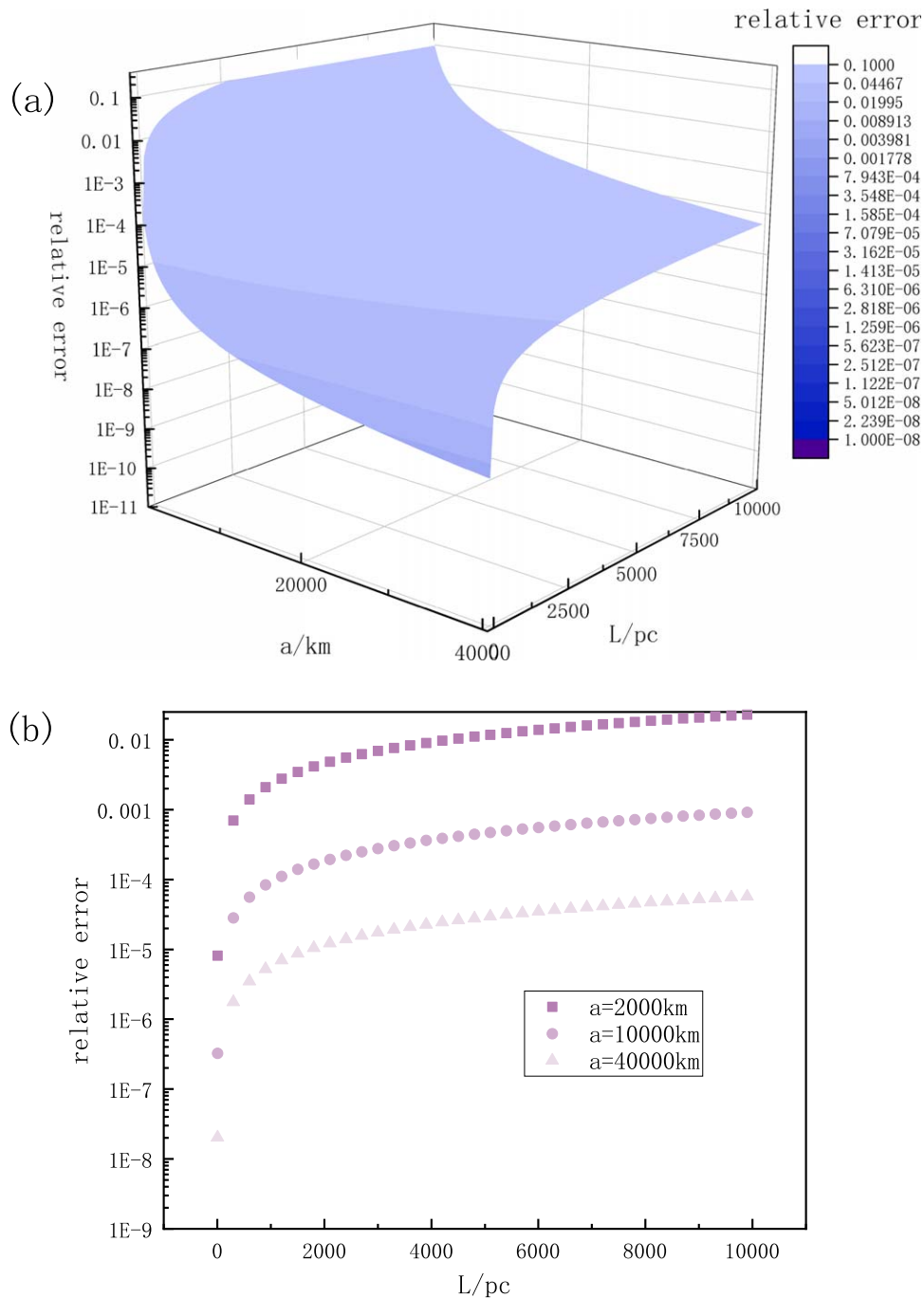


**Figure 4.** (a) The distribution of the relative error, stellar distance ( $L$ ) and baseline length ( $a$ ). The measurement accuracy is set as  $\Delta t = 10^{-18}$  s). Logarithmic coordinates are used for relative errors. (b) The trend of relative error with stellar distance when the baseline length is 2000 km, 10,000 km and 40,000 km, from top to bottom respectively. The relative error decreases with the length of the base station and increases with the distance from the star. When the star is 10 kpc away and the baseline distance ( $a$ ) is 2000 km, the relative error is within 3%.

We should mention that logarithmic coordinate is used to analyze relative error and the measurement accuracy is set as  $\Delta t = 10^{-18}$  s. The upper panel is a three-dimensional diagram and panel (b) shows the distribution between relative error and stellar distance when the baseline length is 2000 km,

10,000 km and 40,000 km, from top to bottom respectively. The stellar distance extends out to 10 kpc. We can see the relative error increases along with stellar distance  $L$ , and decreases with the increase of baseline length  $a$ . When the star is 10 kpc away and the baseline distance is 2000 km, the

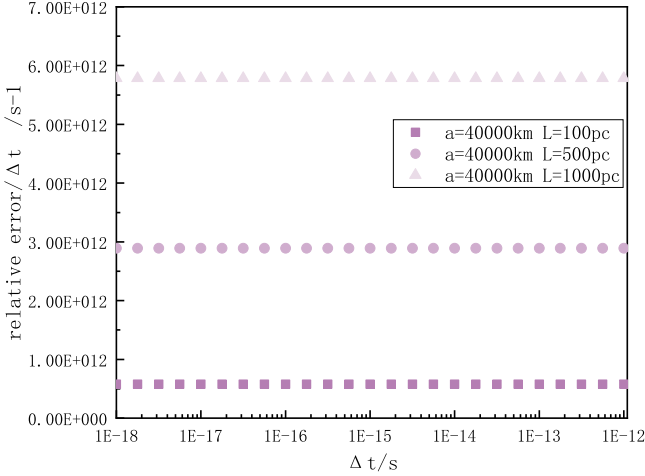


**Figure 5.** The trend in the ratio of the relative error to the precision of time measurement  $\Delta t$  with different  $\Delta t$ . When the baseline length ( $a$ ) and the stellar distance ( $L$ ) are determined, the relative error of ranging is proportional to the precision of time measurement.

ranging error is about 232 pc and the relative error is within 3%. The error can become lower by extending the baseline length. As mentioned before, Gaia can determine distances to stars out to 30,000 ly, i.e 10 kpc, with a precision of up to  $0''.00001$ . and we can know the relative error is approximately 8%.

Figure 5 features the trend of the relative error with stellar distance ( $L$ ) and  $\Delta t$ . Baseline length ( $a$ ) is set as 20,000 km. We can see relative error will increase by one order of magnitude with each order of magnitude increase in the stellar distance ( $L$ ). This result is consistent with what is shown in Figure 4(b).

We can see that our ranging method has the advantage of higher measurement accuracy. Moreover, because it is only restricted by time accuracy, it can theoretically measure farther distances. Currently, the best time measurement accuracy is  $\Delta t = 1$  as. Assuming we select three base stations on the Earth at a distance of 2000 km and measure the distance to Betelgeuse, which is 640 ly away from us, the ranging error is only 0.29 ly and relative error is within 0.045%. If we can extend the baseline length (like using a geosynchronous orbit (40,000 km)), and improve the time measurement accuracy to  $\Delta t = 1$  fs, the relative error can be lower and within 0.11%.

Above all, the measurement can be improved by a couple of orders of magnitude by changing to a better clock, expanding the baseline length or just using more base stations. It is worth mentioning that clocks with an accuracy of  $10^{-19}$  s have been prepared (Campbell et al. 2017). The huge development potential is inestimable. In practical situations, existing base stations can be selected, as long as the relative position relationship between them is known. In addition, the influence of other error sources on ranging accuracy can be reduced as much as possible by selecting the appropriate time to measure the range.

## 2.5. Other Ranging Methods

In 2.3, we put forward a ranging method based on the assumption that the station distribution is strictly equidistant, and analyzed its ranging accuracy in 2.4. In practical work, we can choose existing base stations for the ranging measurement, as long as these base stations can carry out second-order correlation measurement.

Assuming that there are  $N$  base stations selected for the ranging measurement, the connection between these base stations can form a series of baselines  $L$ , and the number of baselines is  $\frac{N*(N-1)}{2}$ . Generally, the locations of these base stations are known, so we do not have to measure the length of these baselines. For a particular baseline  $L_{ij}$  with base station  $i$  and base station  $j$  as endpoints, a time delay  $\tau_{ij}$  can be measured by using second-order correlation measurement. For the  $\frac{N*(N-1)}{2}$  baselines, the number of independent time delays obtained by measuring  $g^{(2)}$  is  $n$ .  $n \leq \frac{N*(N-1)}{2}$  and  $n$  will not always be equal to the baseline number  $\frac{N*(N-1)}{2}$  because some time delays can be determined from the time delay acquired from other baselines. Considering these independent time delays, we can know the optical path difference between the star and each base station. Thus, we can use the base station locations to calculate the distance to the stars. We note that this method can be utilized to measure not only the distance of stars, but also the position of stars. Each independent time delay will reduce one degree of freedom of the star's position. When the star's position is fully determined, the remaining independent time delay can also be added to the calculation to reduce the uncertainty in the position. Similar methods of position calculation relying on time delays are widely employed in very long baseline interferometry (VLBI, Sekido & Fukushima 2006; Liao et al. 2014) and other astronomical observations.

## 3. Principal Experiment

We have completed an experiment to demonstrate the feasibility of measuring differences in distance. The experimental setup is illustrated in Figure 6. The 405 nm pump light coming from the laser passes through HWP and PBS successively. The coherence length of our laser is more than 3 meters. Then we adjust power so as to convert the photon into a horizontally polarized state  $|H\rangle$ . After focusing light onto a PPKTP crystal, we successfully obtained the 810 nm entangled photon pair with orthogonal polarization state by using SPDC process where polarization states are horizontal polarization  $|H\rangle$  and vertical polarization  $|V\rangle$ . By utilizing a longpass filter to filter out the pump light of 405 nm, finally we have a pair of 810 nm photons produced at the same time. Therefore, our device could be used as a source of entangled photon pairs.

The photon pair is divided in two ways (A and B), according to polarization after passing through PBS, and is received respectively by observers at A and B. As we mentioned before,

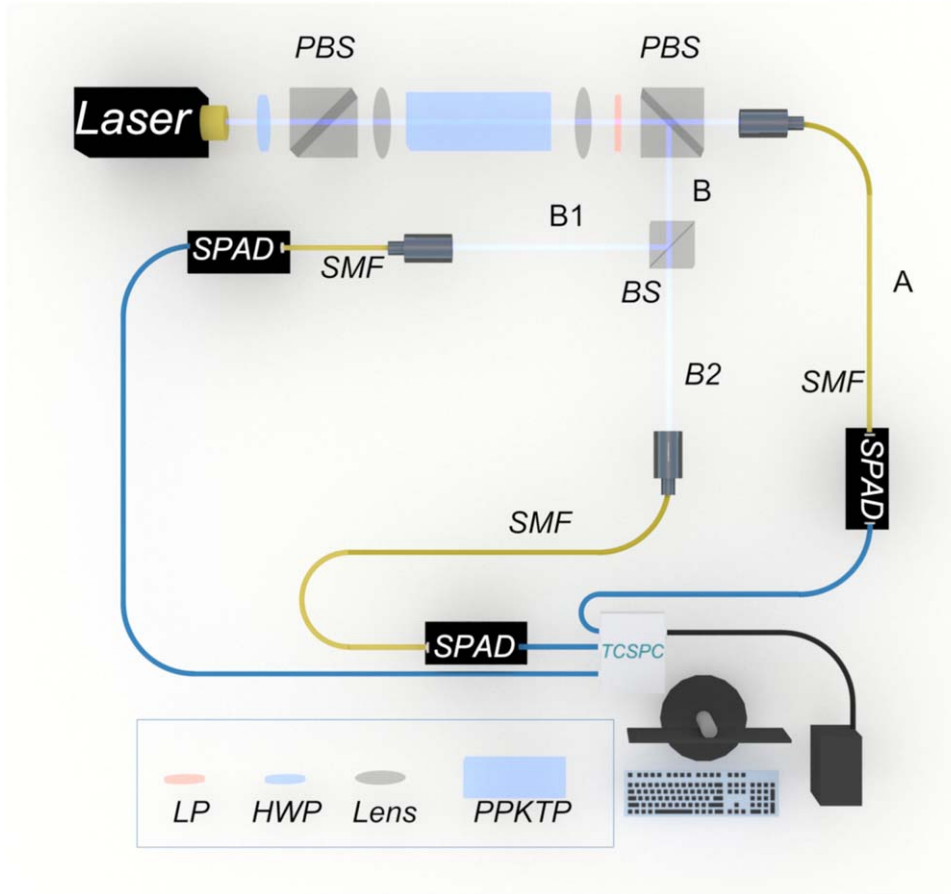


**Figure 6.** Experimental schematic diagram. A heralded single photon source was used. TCSPC was utilized to measure the second order correlation  $g^{(2)}$ . By adding an additional fiber to B2, the optical path difference between B1 and B2 can be changed. B1 and B2 represent two base stations. From the offset distance of the abscissa of  $g^{(2)}$  curve peak, we can get the optical path difference between B1 and B2 caused by the additional fiber. According to the ranging principle, we can range the star as long as we know the optical path difference between the base stations.

entangled photons must appear simultaneously. So if observer A receives a photon at some time, B will receive the other photon accordingly. In this way, we successfully prepared a heralded single photon source.

If we do not detect single photon observer A and only use B to receive the light signal, now observer B receives thermal light instead of the heralded single photon source. Thus, our device could prepare the thermal light, single photon and entangled photon pair. Since the  $g^{(2)}$  functions of three sources are not equal to 1, we can determine the distance difference according to the previous theory. We propose our ranging scheme based on that.

We divide the signal light into B1 and B2 by BS, then use the single photon detector to detect the signal, counting B2 and B1 signals as the START and STOP signal of time-correlated single-photon counting (TCSPC) respectively (Phillips et al. 1985). The statistical distribution of the optical field signal we obtained is displayed in Figure 7.

If we extend the optical path difference between B1 and B2 by setting up a roughly 159 cm section of fiber on B2, we can gain the following results after repeating the above operation with TCSPC. As we can see in Figure 8, the peak of the  $g^{(2)}$  curve shifts from 157.77 to 280.21 bin. The refractive index of the fiber we used is  $n_g = 1.4735$ .

So, it is easy to calculate the length of the fiber

$$l = (280.21 - 157.77) \text{ bin} \times 64 \text{ ps} \times 2.034 \times 10^8 \text{ m s}^{-1} \approx 159.39 \text{ cm}. \quad (10)$$

In this experiment, the time resolution of TCSPC is 64 ps, so the upper limit of theoretical resolution is

$$64 \text{ ps} \times 2.034 \times 10^8 \text{ m s}^{-1} \approx 1.30 \text{ cm}. \quad (11)$$

Compared with the actual length of the fiber, we demonstrate that the optical path difference can be measured from the  $g^{(2)}$  curve shift.

In addition, if the source is a single photon source or entangled source, we can also achieve the measurement of fiber

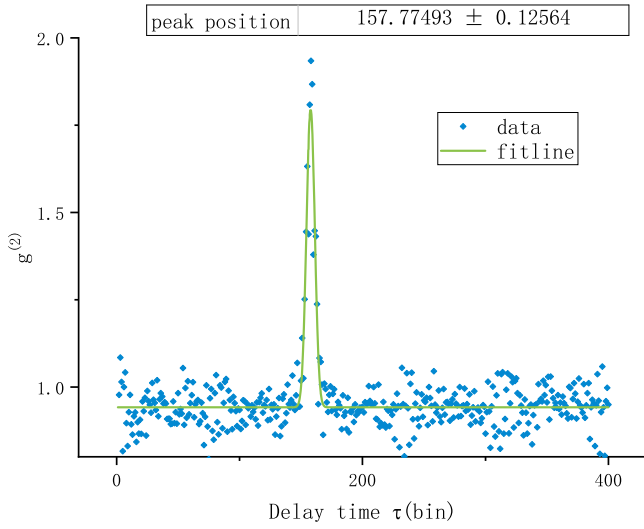


**Figure 7.**  $g^{(2)}$  between B1 and B2 (without additional fiber).

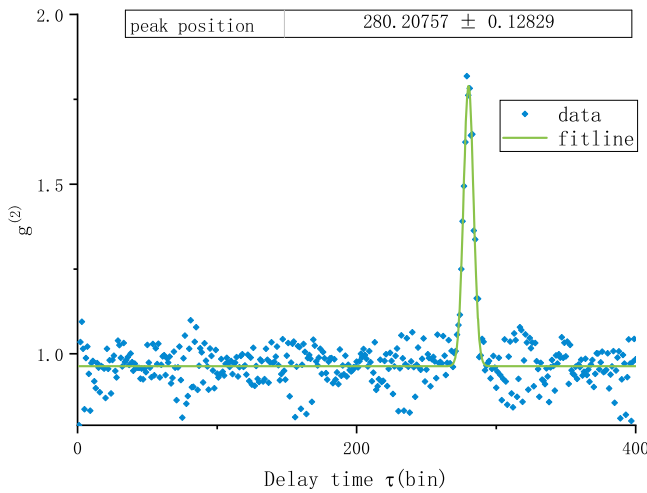


**Figure 8.**  $g^{(2)}$  between B1 and B2 (with additional fiber). Compared with Figure 7, the second-order correlation function is shifted to the right by 122.44 bins, which corresponds to the optical path difference introduced by the additional fiber.

length difference, and the result is consistent with the above conclusion. In other words, the scheme we proposed could realize the measurement of the distance difference between the light source and observers as long as the source does not emit a laser, for which  $g^{(2)}$  equals 1. After measuring the distance difference between the source and observers ( $L_B$ ,  $L_C$ ), we can calculate the distance to the star ( $L$ ) by relying on formula (7).

This experiment demonstrates the feasibility of the theoretical scheme for measuring the optical path difference and confirms that the brightness of the star does not need to be too

high because the optical path difference of a single photon can still be detected in the experiment.

## 4. Conclusions

In this paper, we propose the stellar ranging scheme based on second order correlation measurement for the first time, applying the second order correlation theory of a light field to stellar ranging, and carrying out the primary demonstration and the verification experiment based on an SPDC light source. Compared with the traditional method of trigonometric parallax ranging, we confirm that our scheme has many advantages.

This method is based on second order correlation theory, and its accuracy only depends on the accuracy of time measurement, so it does not require a parallax angle measurement. Then the objects of this scheme can be thermal sources or other sources that emit non-classical light. From the summary above, we can say that the scheme has overcome the limitation of emission power on the measurement distance, so its range is much larger than active ranging. Apart from this, it also has good resistance to external noise, random signal interference and requires lower cost and shorter time. Furthermore, since the error of stellar ranging is directly proportional to the time accuracy and inversely proportional to the square of the distance between the observers, we may improve the measurement range and accuracy by changing to a better clock and extending the baseline length in the future. As long as the light emitted by a star can be received by observers, we can implement such a process.

## Acknowledgments

This work is supported by National Key Research and Development Program Earth Observation and Navigation Key Specialities (No. 2018YFB0504300).

## ORCID iDs

Can Xu,  <https://orcid.org/0000-0002-8437-6659>

## References

- Boitier, F., Godard, A., Rosencher, E., & Fabre, C. 2009, *NatPh*, **5**, 267
- Burnham, D. C., & Weinberg, D. L. 1970, *PhRvL*, **25**, 84
- Campbell, S. L., Hutson, R. B., Marti, G. E., et al. 2017, *Sci*, **358**, 90
- Chang, D. E., Vuletić, V., & Lukin, M. D. 2014, *NaPho*, **8**, 685
- Gaia Collaboration, Brown, A. G. A., Vallenari, A., et al. 2021, *A&A*, **649**, A1
- Gatti, A., Brambilla, E., & Lugiato, L. A. 2003, *PhRvL*, **90**, 133603
- Giovannetti, V., Lloyd, S., & Maccone, L. 2001, *Natur*, **412**, 417
- Giovannetti, V., Lloyd, S., & Maccone, L. 2002, *PhRvA*, **65**, 022309
- Giovannetti, V., Lloyd, S., & Maccone, L. 2004, *Sci*, **306**, 1330
- Glauber, R. J. 1963a, *PhRv*, **131**, 2766
- Glauber, R. J. 1963b, *PhRvL*, **10**, 84
- Glauber, R. J. 1963c, *PhRv*, **130**, 2529
- Goodman, J. W. 2007, in *Speckle Phenomena in Optics: Theory and Applications* Speckle Phenomena in Optics: Theory and Applications, ed. J. W. Goodman (Greenwood Village, CO: Roberts and Company)
- Hanbury Brown, R. 1956, *Natur*, **178**, 1046

- Karmakar, S., Zhai, Y.-H., Chen, H., & Shih, Y. 2011, CLEO:2011—Laser Applications to Photonic Applications (Optical Society of America), QFD3
- Kwiat, P. G., Mattle, K., Weinfurter, H., et al. 1995, *PhRvL*, **75**, 4337
- Liao, S.-L., Tang, Z.-H., & Qi, Z.-X. 2014, *RAA*, **14**, 1029
- Ling, A., Lamas-Linares, A., & Kurtsiefer, C. 2008, *PhRvA*, **77**, 043834
- Liu, X.-F., Chen, X.-H., Yao, X.-R., et al. 2014, *OptL*, **39**, 2314
- Madore, B. F., & Freedman, W. L. 1998, *ApJ*, **492**, 110
- Maíz Apellániz, J., Pantaleoni González, M., Barbá, R. H., et al. 2018, *A&A*, **616**, A149
- Mandel, L., & Wolf, E. 1995, *Optical Coherence and Quantum Optics* (Cambridge: Cambridge Univ. Press)
- Mignard, F. 2019, *CRPhy*, **20**, 140
- Phillips, D., Drake, R. C., O'Connor, D. V., & Christensen, R. L. 1985, *IS&T*, **14**, 267
- Reid, M. J., Menten, K. M., Brunthaler, A., et al. 2014, *ApJ*, **783**, 130
- Reid, M. J., Menten, K. M., Zheng, X. W., et al. 2009, *ApJ*, **700**, 137
- Sekido, M., & Fukushima, T. 2006, *J. Geod.*, **80**, 137
- Smith, H. J., & Eichhorn, H. 1996, *MNRAS*, **281**, 211
- Thorn, J. J., Neel, M. S., Donato, V. W., et al. 2004, *AmJPh*, **72**, 1210
- Valencia, A., Chekhova, M. V., Trifonov, A., & Shih, Y. 2002, *PhRvL*, **88**, 183601
- Zhang, B., Zheng, X., Reid, M. J., et al. 2017, *ApJ*, **849**, 99
- Zhu, J., Chen, X., Huang, P., & Zeng, G. 2012, *ApOpt*, **51**, 4885
- Zhu, J., Huang, P., Xiao, X., & Zeng, G. 2013, *ApOpt*, **43**, 373